Reprinted from

MATERIALS SCIENCE AND ENGINEERING

ELSEVIER PUBLISHING COMPANY
AMSTERDAM

Slip-Induced Directional Order Theory for $B2$-Type Superlattices

G. Y. CHIN

Bell Telephone Laboratories, Incorporated, Murray Hill, N.J. (U.S.A.)

(Received January 7, 1966; revised February 16, 1966)

SUMMARY

The theory of slip-induced directional order has been developed for the B2*-type superlattices. The treatment is based on the original work of Chikazumi* et al. *Separate analyses have been made for slip on* {110} ⟨111⟩ *and* {112} ⟨111⟩ *systems, which are prominent slip systems in b.c.c. alloys. In addition, consideration has been made for both long- and short-range order in the structure, as well as for nearest-neighbor and next-nearest-neighbor interactions.*

The results of the analysis are summarized as follows: (1) *In the case of nearest-neighbor interactions,* (a) {110} ⟨111⟩ *slip in both long- and short-range ordered lattices results in the slip plane normal as the effective direction of excess* like-atom *pairs*; (b) {112} ⟨111⟩ *slip, on the other hand, results in the slip direction as the effective direction of* unlike *pairs.* (2) *In the case of next-nearest-neighbor interactions,* (a) {110} ⟨111⟩ *slip in both long- and short-range ordered lattices leads to that* ⟨100⟩ *direction which lies on the slip plane, as the effective like-pair direction, while* (b) *no anisotropy is expected from slip in* {112} ⟨111⟩ *systems.*

The theory is applied to FeCo, whereby the magnetic anisotropy energy obtained by rolling single crystals of (001)[$\bar{1}$10], (115)[$\bar{1}$10], (112)[$\bar{1}$10], (111) [$\bar{1}$10] *and* (110) [$\bar{1}$10] *orientations are calculated. Except for* (110) [$\bar{1}$10], *these orientations comprise the crystallographic texture spread as found in heavily rolled polycrystalline material near the FeCo composition. The results of the calculations are in good agreement with the observations of Fahlenbrach* et al. *if mixed slip of both* {110}⟨111⟩ *and* {112}⟨111⟩ *slip systems (pencil glide) is assumed to take place during deformation. Such mixed slip has been observed by Stoloff and Davies.*

Possible contributions from magnetocrystalline and magnetostrictive anisotropies to the observed results of rolled FeCo are also discussed.

RÉSUMÉ

L'auteur a élaboré une théorie de l'ordre directionnel créé par la déformation par glissement dans les surstructures de type B2. *Son calcul repose sur le modèle théorique proposé initialement par Chikazumi* et al. *Il a analysé séparément les cas où le glissement actif est* {110}⟨111⟩ *et* {112}⟨111⟩; *ces deux systèmes sont en effet les systèmes de glissement prédominants dans les alliages de structure cubique centrée. De plus il a considéré à la fois les situations où la structure possédait un ordre à grande distance et celles où elle était caractérisée par un ordre à courte distance et il a fait intervenir aussi bien les interactions entre premier voisins que celles entre seconds voisins.*

Les résultats de cette analyse peuvent être résumés de la manière suivante: (1) *Si l'on considère seulement les interactions entre premiers voisins,* (*a*) *le glissement du système* {110}⟨111⟩ *aboutit à la création dans les structures ordonnées d'un excédent de* paires d'atomes semblables *dans la direction perpendiculaire au plan de glissement, que l'ordre soit à grande distance ou à courte distance*; (*b*) *par contre le glissement du système* {112}⟨111⟩ *aboutit à la formation d'un excédent de* paires d'atomes dissemblables *dans la direction de glissement.* (2) *Si l'on tient compte des interactions entre seconds voisins,* (*a*) *le glissement* {110} ⟨111⟩ *conduit à un excédent de paires d'atomes semblables dans celle des directions* ⟨100⟩ *qui est contenue dans le plan de glissement, dans le cas de l'ordre à grande distance aussi bien que dans celui de l'ordre à courte distance, tandis que* (*b*) *on ne doit s'attendre à*

and $[1\bar{1}1]$) that lie on the (110) slip plane, we still have four AB pairs each. On the other hand, along $[\bar{1}\bar{1}1]$ and [111], which lie on the $(1\bar{1}0)$ plane, we now have two AA pairs and two BB pairs. Hence, we gain two BB pairs each along $[\bar{1}\bar{1}1]$ and [111]. If there is partial ordering, as expressed by the LRO parameter s, $\Delta N_{BB}=2s^2$ (see Appendix). Since the area of (110) planes in Fig. 1 is $2a^2\sqrt{2}$, we have $\Delta N_{BB}=s^2/a^2\sqrt{2}$ per unit (110) area. In addition, as discussed by Chikazumi *et al.*[1], this quantity is obtained by assuming that an *odd* number of *unit* dislocations have passed on each *slipped* plane. Thus, we insert a factor of $\frac{1}{2}$ for the chance that an odd number of dislocations had passed, and a factor p_0 for the probability that a unit dislocation is not paired with another to form a superdislocation, as it tends to do when long-range order is present. Finally, the number of slip planes (per unit distance perpendicular to the slip plane) that have *slipped* is equal to $|\gamma|/nb$ where γ is the macroscopic glide-shear resulting from the slip, n is the average number of dislocations passed per *slipped* plane, and $b=a\sqrt{3}/2$ is the Burger's vector. Thus, per unit volume,

$$\Delta N_{BB}=\frac{p_0}{2}\frac{s^2}{a^2\sqrt{2}}\frac{|\gamma|}{nb}=\frac{Np_0s^2|\gamma|}{2\sqrt{6n}}, \qquad (2)$$

where $N=2/a^3$ is the number of atoms per unit volume. Equation (2) can be converted to Chikazumi's notation by letting $p'=1/n$ as the probability of passing a dislocation per atomic (slip) plane, and noting that $\gamma=Sb/d$ where S is the "slip density", or the average (effective) number of dislocations passed per atomic (slip) plane, and $d=a/\sqrt{2}$ is the slip plane spacing. Then eqn. (2) becomes

$$\Delta N_{BB}=\tfrac{1}{4}Np_0p's^2S. \qquad (3)$$

Since the directions of the BB pairs thus induced by (110) $[\bar{1}11]$ slip are $[\bar{1}\bar{1}1]$ and [111], eqn. (1) becomes

$$E=\tfrac{1}{4}Nlp_0p's^2S\left[\left(-\frac{1}{\sqrt{3}}\alpha_1-\frac{1}{\sqrt{3}}\alpha_2+\frac{1}{\sqrt{3}}\alpha_3\right)^2+\left(\frac{1}{\sqrt{3}}\alpha_1+\frac{1}{\sqrt{3}}\alpha_2+\frac{1}{\sqrt{3}}\alpha_3\right)^2\right]=$$
$$=\tfrac{1}{3}Nlp_0p's^2S(\alpha_1\alpha_2)+\text{const}, \qquad (4)$$

where α_1, α_2, α_3 are the direction cosines of the local magnetization vector with respect to the cubic axes. The functional dependence $\alpha_1\alpha_2$ in eqn. (4) means that the slip plane normal [110] is the effective BB pair direction. (It may also be deduced from the fact that [110] is symmetrically disposed (at an angle $<45°$) with respect to $[\bar{1}\bar{1}1]$ and [111].) Hence, in accordance with the assumption $Nl<0$, the slip plane normal becomes an easy axis of magnetization as a result of slip.

In the general case where n_{1i}, n_{2i}, n_{3i} are the direction cosines of the slip plane normal of the ith system, we have

$$E=\tfrac{2}{3}Nlp_0p's^2\sum_i|S_i|(n_{1i}n_{2i}\alpha_1\alpha_2+n_{2i}n_{3i}\alpha_2\alpha_3+n_{3i}n_{1i}\alpha_3\alpha_1), \qquad (5)$$

where the summation is carried over all active slip systems i.

For the case of short range order, the directions of BB pairs induced by $(110)[\bar{1}11]$ slip are again $[\bar{1}\bar{1}1]$ and [111]. It turns out that in the two unit cells of Fig. 1a, the number of BB pairs in each $\langle 111\rangle$ direction before slip is $1-\sigma$, where σ is the Bethe short-range order parameter (see Appendix). According to Cohen and Fine[12], the structure across the slip planes becomes random after three or four slip steps. Hence we may take $\sigma=0$ after slip, so that the number of BB pairs gained by slip is $\sqrt{2}\sigma/4a^2$ per unit (110) area. To this we multiply by $|\gamma|/nb$, the effective number of *slipped* planes (per unit distance perpendicular to the slip plane). Thus

$$\Delta N_{BB}=\frac{\sqrt{2}\sigma|\gamma|}{4na^2b}=\tfrac{1}{4}Np'\sigma S, \qquad (6)$$

with the direction cosines of the BB pairs the same as the LRO case. By combining eqns. (5) and (6), we finally obtain the induced uniaxial anisotropy energy

$$E_{NN}=\tfrac{2}{3}E_1\sum_i|S_i|(n_{1i}n_{2i}\alpha_1\alpha_2+n_{2i}n_{3i}\alpha_2\alpha_3+n_{3i}n_{1i}\alpha_3\alpha_1), \qquad (7)$$

where $E_1\equiv Nlp'(p_0s^2+\sigma)$, and the subscript NN denotes the nearest neighbor case.

(*b*) *Next-nearest-neighbor (NNN) interactions*

In the body-centered cubic structure, the distance between next nearest neighbors is only 13.5% greater than that between nearest neighbors; hence NNN interactions may become important, especially in certain symmetric orientations where NN contributions to the slip-induced anisotropy become small.

In the undeformed state with complete LRO, the NNN $\langle 100\rangle$ directions contain 2AA+2BB pairs in the two unit cells of Fig. 1(a). After (110) $[\bar{1}11]$ slip, Fig. 1(b), the [001] direction which lies on the slip plane, is undisturbed. The [100] and [010] directions, on the other hand, now contain four AB pairs each. Hence the slip has resulted in a (negative) gain of -2 BB pairs. For partial LRO, $\Delta N_{BB} = -2s^2$ (see Appendix), or $-s^2/a^2\sqrt{2}$ per (110) area. Multiplying by the appropriate factors as in eqns. (2) and (3), we obtain, per unit volume,

$$\Delta N_{BB} = -\tfrac{1}{4}Np_0p's^2S \qquad (8)$$

in both [001] and [010] directions. Thus, from eqn. (1),

$$\begin{aligned} E &= -\tfrac{1}{4}Nl_2p_0p's^2S[(1\cdot\alpha_1+0\cdot\alpha_2+0\cdot\alpha_3)^2 \\ &\quad +(0\cdot\alpha_1+1\cdot\alpha_2+0\cdot\alpha_3)^2] \\ &= -\tfrac{1}{4}Nl_2p_0p's^2S(\alpha_1^2+\alpha_2^2) \\ &= \tfrac{1}{4}Nl_2p_0p's^2S\alpha_3^2\,, \end{aligned} \qquad (9)$$

where l_2 refers to the value of l for NNN pairs. The functional dependence of eqn. (9) indicates that the [001] direction, which lies on the slip plane (110), is the effective BB pair direction. If the value of l_2 is assumed negative, by analogy with l, [001] is an easy axis of magnetization. In the general case, we have

$$E = \tfrac{1}{4}Nl_2p_0p's^2\sum_i|S_i|(\delta_{1i}^2\alpha_1^2+\delta_{2i}^2\alpha_2^2+\delta_{3i}^2\alpha_3^2)\,, \qquad (10)$$

where δ_{1i}, δ_{2i}, δ_{3i} are the direction cosines of the $\langle 100\rangle$ direction lying on the ith $\{110\}$ slip plane.

For the case of short-range order, the (negative) gain in BB pairs along [100] or [010] is $-\sigma_2/2\sqrt{2a^2}$ per unit (110) slipped area (see Appendix), where σ_2 is the Bethe SRO parameter for NNN pairs. After inserting the appropriate factors as in eqn. (6) and combining the direction cosines as in eqn. (10), the expression of E for the SRO case becomes

$$E = \tfrac{1}{4}Nl_2p'\sigma_2\sum_i|S_i|(\delta_{1i}^2\alpha_1^2+\delta_{2i}^2\alpha_2^2+\delta_{3i}^2\alpha_3^2)\,. \qquad (11)$$

The combined results of eqns. (10) and (11) then lead to a slip-induced anisotropy energy of

$$E_{NNN} = \tfrac{1}{4}E_2\sum_i|S_i|(\delta_{1i}^2\alpha_1^2+\delta_{2i}^2\alpha_2^2+\delta_{3i}^2\alpha_3^2)\,, \qquad (12)$$

where $E_2 \equiv Nl_2p'(p_0s^2+\sigma_2)$, for the next nearest-neighbor case.

(c) *Applications to rolling*

Equations (7) and (12) have been applied to calculate the slip-induced anisotropy obtained by rolling single crystals. As Fig. 2 shows, the rolled texture of an alloy near the 50% Fe–50% Co composition may be considered as a band of orientations $\{001\}$ to $\{111\}\langle\bar{1}10\rangle$, that is, the rolling direction is a $\langle\bar{1}10\rangle$ orientation, but the rolling plane consists of a continuous rotation about $\langle\bar{1}10\rangle$, from $\{001\}$ to $\{111\}$ positions. Hence calculations were made for $(001)[\bar{1}10]$, $(115)[\bar{1}10]$, $(112)[\bar{1}10]$, and $(111)[\bar{1}10]$ orientations which comprise the texture spread. (For completeness, the $(110)[\bar{1}10]$ orientation was also analyzed.) It may be added that the rolled texture of Fig. 2 is common to most b.c.c. alloys.

The procedure in the calculations is essentially identical with that adopted previously for $FeNi_3$[4]. In Table I are listed the values of the macroscopic strain components ε_{xx}, ε_{yz} etc. in terms of the slip

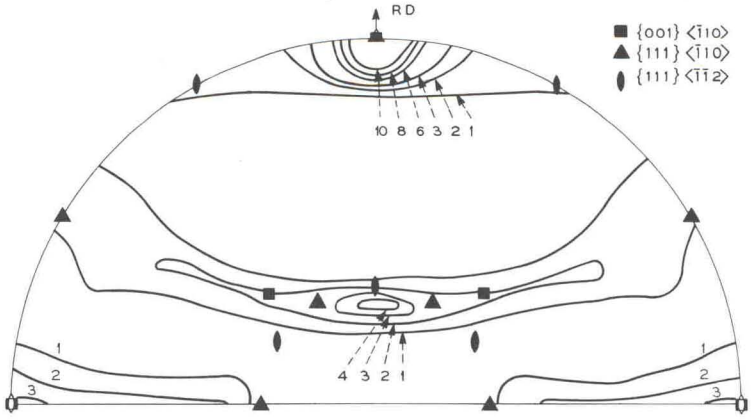

Fig. 2. {110} pole figure of cold-rolled polycrystalline Remendur (49% Fe–49% Co–4% V) after 95% thickness reduction. Ideal texture can be described as {001} to {111} ⟨1̄10⟩. (A.T. English and G.Y. Chin, unpublished.)

TABLE I: VALUES OF ε, n AND δ (REFERRED TO CUBIC AXES) FOR THE TWELVE $\{110\}\langle 111\rangle$ SLIP SYSTEMS

No. of slip system	*Slip plane*	*Slip direction*	$2\varepsilon_{xx}$	$2\varepsilon_{yy}$	$2\varepsilon_{zz}$	$4\varepsilon_{yz}$	$4\varepsilon_{zx}$	$4\varepsilon_{xy}$	$2n_1n_2$	$2n_2n_3$	$2n_3n_1$	δ_1^2	δ_2^2	δ_3^2
1	$(01\bar{1})$	$[111]$	0	S_1	$-S_1$	0	$-S_1$	S_1	0	-1	0	1	0	0
2	$(10\bar{1})$	$[111]$	S_2	0	$-S_2$	$-S_2$	0	S_2	0	0	-1	0	1	0
3	$(1\bar{1}0)$	$[111]$	S_3	$-S_3$	0	$-S_3$	S_3	0	-1	0	0	0	0	1
4	(101)	$[11\bar{1}]$	S_4	0	$-S_4$	S_4	0	S_4	0	0	1	0	1	0
5	(011)	$[11\bar{1}]$	0	S_5	$-S_5$	0	S_5	S_5	0	1	0	1	0	0
6	$(1\bar{1}0)$	$[11\bar{1}]$	S_6	$-S_6$	0	S_6	$-S_6$	0	-1	0	0	0	0	1
7	(110)	$[1\bar{1}1]$	S_7	$-S_7$	0	S_7	S_7	0	1	0	0	0	0	1
8	$(10\bar{1})$	$[1\bar{1}1]$	S_8	0	$-S_8$	S_8	0	$-S_8$	0	0	-1	0	1	0
9	(011)	$[1\bar{1}1]$	0	$-S_9$	S_9	0	S_9	S_9	0	1	0	1	0	0
10	$(01\bar{1})$	$[\bar{1}11]$	0	S_{10}	$-S_{10}$	0	S_{10}	$-S_{10}$	0	-1	0	1	0	0
11	(101)	$[\bar{1}11]$	$-S_{11}$	0	S_{11}	S_{11}	0	S_{11}	0	0	1	0	1	0
12	(110)	$[\bar{1}11]$	$-S_{12}$	S_{12}	0	S_{12}	S_{12}	0	1	0	0	0	0	1

TABLE II: SUMMARY OF RESULTS BASED ON $\{110\}\langle 111\rangle$ SLIP

Rolling plane	*Rolling direction*	*Active slip systems*	$\lvert S_i\rvert$	E_{NN}	*Easy* axis*	E_{NNN}	*Easy* axis*
(001)	$[\bar{1}10]$	8,9,10,11	$r/2$	0	—	$-(\frac{1}{4}E_2r)\alpha_3^2$	RD+TD
(115)	$[\bar{1}10]$	4,5,8,9,10,11	$\lvert S_4\rvert=\lvert S_5\rvert=2r/27$ $\lvert S_8\rvert=\lvert S_{10}\rvert=r/6$ $\lvert S_9\rvert=\lvert S_{11}\rvert=5r/6$	$(\frac{20}{81}E_1r)[\alpha_3(\alpha_1+\alpha_2)]$	RPN	$-(\frac{29}{108}E_2r)\alpha_3^2$	RD
(112)	$[\bar{1}10]$	4,5,9,11	$\lvert S_4\rvert=\lvert S_5\rvert=r/3$ $\lvert S_9\rvert=\lvert S_{11}\rvert=r$	$(\frac{4}{9}E_1r)[\alpha_3(\alpha_1+\alpha_2)]$	RPN	$-(\frac{1}{3}E_2r)\alpha_3^2$	RD
(111)	$[\bar{1}10]$	1,2,4,5,9,11	$\lvert S_1\rvert=\lvert S_2\rvert=r/6$ $\lvert S_4\rvert=\lvert S_5\rvert=r/2$ $\lvert S_9\rvert=\lvert S_{11}\rvert=r$	$(\frac{4}{9}E_1r)[\alpha_3(\alpha_1+\alpha_2)]$	RPN	$-(\frac{5}{12}E_2r)\alpha_3^2$	RD
(110)	$[\bar{1}10]$	1,2,4,5,8,9,10,11	$r/2$	0	—	$-(\frac{1}{2}E_2r)\alpha_3^2$	RD+RPN

* Relative among the three symmetry directions of rolled strip.
RP-rolling plane, RD-rolling direction, RPN-rolling plane normal.

density $|S_i|$ for the twelve $\{110\}\langle 111\rangle$ slip systems. These values are referred to cubic axes of the crystal and were computed from the equation

$$\varepsilon_{ij} = \frac{\gamma}{2}(n_i d_j + n_j d_i) \qquad i,j = x,y,z$$

$$= \frac{\sqrt{6}}{4} S(n_i d_j + n_j d_i)\,, \tag{13}$$

where γ is the glide-shear, and n_i and d_i are the direction cosines of the slip plane normal and the slip direction, respectively. (See Appendix, ref. 4.) Values of (n_{1i}, n_{2i}, n_{3i}) and $(\delta_i, \delta_{2i}, \delta_{3i})$ for use in eqns. (7) and (12) are also included in Table I.

For a given crystal orientation, the method of Bishop and Hill[13,14] is used as a first step to determine which of the 12 possible $\{110\}\langle 111\rangle$ slip systems must operate to accommodate the (rolling) deformation. Next, the macroscopic strain components referred to specimen axes* are converted to those referred to cubic axes by the appropriate coordinate transformation. Table I can then be used to relate the strain components (now referred to cubic axes) and the slip density S_i of the active slip systems which have been determined by the Bishop and Hill method. Finally, the values of S_i for use in eqns. (7) and (12) are solved in terms of the strain components.

It may be noted that for $\{110\}\langle 111\rangle$ slip in b.c.c. alloys, the slip planes and slip directions are merely interchanged from those of $\{111\}\langle 110\rangle$ slip

* If 1, 2, 3 refer to the rolling plane normal, transverse direction, and rolling direction of the specimen respectively, the strain components during rolling are given by $\varepsilon_{11}=-\varepsilon_{33}$, $\varepsilon_{22}=0$, $\varepsilon_{23}=\varepsilon_{31}=\varepsilon_{12}=0$.

in the f.c.c. case. Hence the steps in the calculations are identical in both cases. Since these steps have been followed in detail in ref. 4, only the results of the present analysis are presented. They are summarized in Table II.

(*d*) *Comparison with observed results*

Fahlenbrach and co-workers[6-8] have investigated the magnetic anisotropy in rolled Hyperm Co 50 (49% Fe–49% Co–2% V) and Koerzit T (35% Fe–53% Co–8% V–4% Cr). They found that in the heavily rolled condition, the direction of easiest magnetization is the rolling plane normal, the next easy direction is the transverse direction, and the hardest direction is in the rolling direction. Accordingly we calculated from Table II the anisotropy energies in these three directions, for crystals of (001)[$\bar{1}$10], (115)[$\bar{1}$10], (112)[$\bar{1}$10] and (111)[$\bar{1}$10] orientations which comprise the rolled texture (plus (110)[$\bar{1}$10] for completeness). The results are given in Figs. 3 and 4, with the energy in the rolling direction set at zero arbitrarily.

It may be noted in Fig. 3 that in the nearest-neighbor (NN) case, the rolling plane normal is

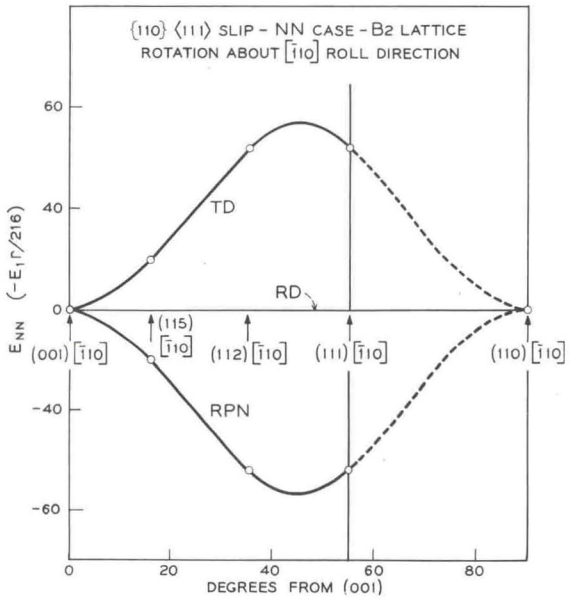

Fig. 3. Calculated slip-induced magnetic anisotropy energy in the three symmetry directions of a rolled strip, as a function of orientation from (001) [$\bar{1}$10] to (110) [$\bar{1}$10]. Curve from (111) [$\bar{1}$10] to (110) [$\bar{1}$10] not applicable for rolled FeCo (see Fig. 2). Calculations based on *nearest-neighbor* interactions, for the case of {110} ⟨111⟩ slip (see Table II). Energy in RD arbitrarily set at zero. Note $E_1 < 0$ for FeCo.

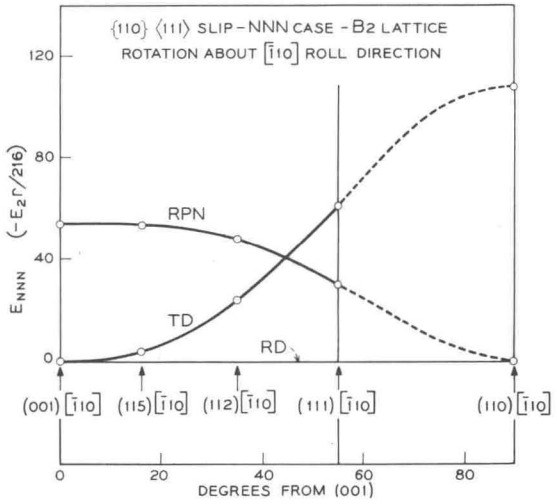

Fig. 4. Same as Fig. 3 except that calculations are based on *next-nearest-neighbor* interactions.

indeed the lowest energy direction as observed by Fahlenbrach *et al.* However, the transverse direction is the hardest, contrary to the observed results. In the (weaker) NNN anisotropy, Fig. 4, the transverse direction is again predicted to be harder than the rolling direction, assuming $l_2 < 0$. Hence it may be concluded that {110}⟨111⟩ slip alone is insufficient to explain the observed anisotropy. It turns out that substantial {112}⟨111⟩ slip is also required. The latter analysis will now be presented.

3. ANALYSIS OF {112}⟨111⟩ SLIP

The case of {112}⟨111⟩ slip is somewhat more complicated than those of {111}⟨110⟩ and {110}⟨111⟩ slip, since the b.c.c. structure repeats itself after every sixth {112} layer. Consequently, the distribution of atom pairs resulting from {112}⟨111⟩ slip generally depends on the arrangement of the slipped planes. Several of these arrangements are shown in Figs. 5 and 6. To a reasonable approximation, one may conclude from examining these arrangements that the effects of {112}⟨111⟩ slip are (1) to convert the three ⟨111⟩ nearest-neighbor directions, other than the slip direction, to an increase of BB (like atom) pairs; and (2) to convert all three ⟨100⟩ next-nearest-neighbor directions to a decrease of BB pairs. The latter effect means that the magnetic anisotropy from NNN interactions may be neglected, and that we may concentrate on the nearest-neighbor case only.

As for the NN case, we again express the mag-

netic anisotropy energy by eqn. (1):

$$E = l\sum_i \Delta N_{BBi}\cos^2\varphi_i\,. \qquad (1)$$

(a) *Long-range order case*

To calculate ΔN_{BBi} in the long-range order case, we note that in a unit cell, the area of any one set of {112} planes is $a^2\sqrt{6}$. In this cell there are eight nearest-neighbor bonds, two each in the four ⟨111⟩ directions. In the fully-ordered, undeformed state, these are AB bonds, *i.e.*, joining an A atom at an α site with a B atom at a β site. We assume, to a reasonable approximation, that after $(\bar{1}12)[1\bar{1}1]$ slip, all odd number of slip steps will convert the two AB bonds to an AA bond plus a BB bond, in all ⟨111⟩ directions except the $[1\bar{1}1]$ slip direction. Hence along [111], $[\bar{1}11]$ or $[11\bar{1}]$, we gain one BB pair. In case of partial LRO, the gain is s^2 (see Appendix). Hence $\Delta N_{BB} = s^2/a^2\sqrt{6}$ per unit $(\bar{1}12)$ area.

As in the previous treatment for {110}⟨111⟩ slip, the complete expression for ΔN_{BB} includes the factor $(1/2)(p_0 p'|S|/d)$, where $d = a/\sqrt{6}$ is the {112} slip plane spacing. Hence, per unit volume,

$$\Delta N_{BB} = \tfrac{1}{2}p_0 p'\left(\frac{\sqrt{6}}{a}\right)\left(\frac{s^2}{a^2\sqrt{6}}\right)|S|$$
$$= \tfrac{1}{4}N p_0 p' s^2 |S|\,. \qquad (14)$$

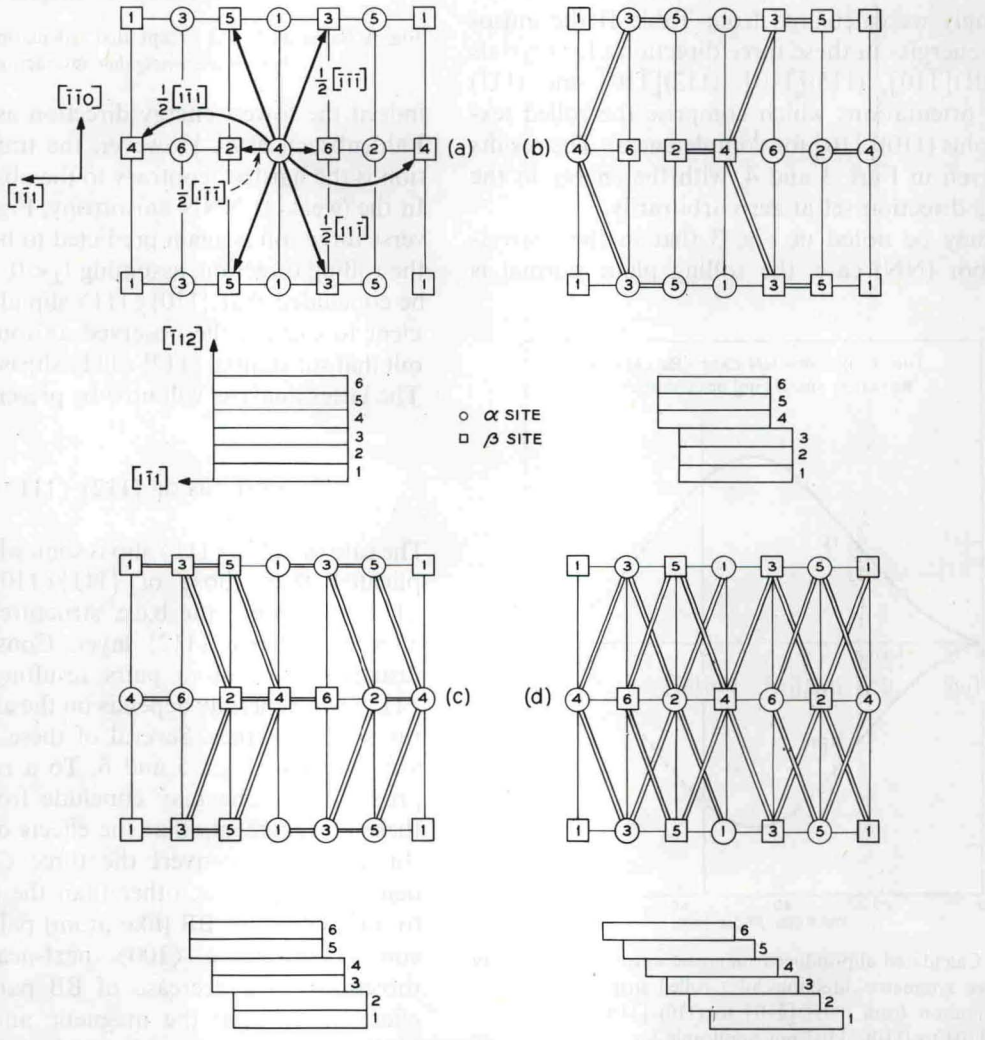

Fig. 5. Atomic arrangement in six consecutive $(\bar{1}12)$ layers of a *B2* superlattice, showing effect of $(\bar{1}12)[1\bar{1}1]$ slip on the distribution of *nearest-neighbor* atom pairs. (a) Undeformed state; all four ⟨111⟩ NN directions contain AB pairs only. (b) to (d) Alternative arrangements after $(\bar{1}12)$ [111] slip, showing AA and BB pairs (double bars) induced in all ⟨111⟩ directions except the $[1\bar{1}1]$ slip direction.

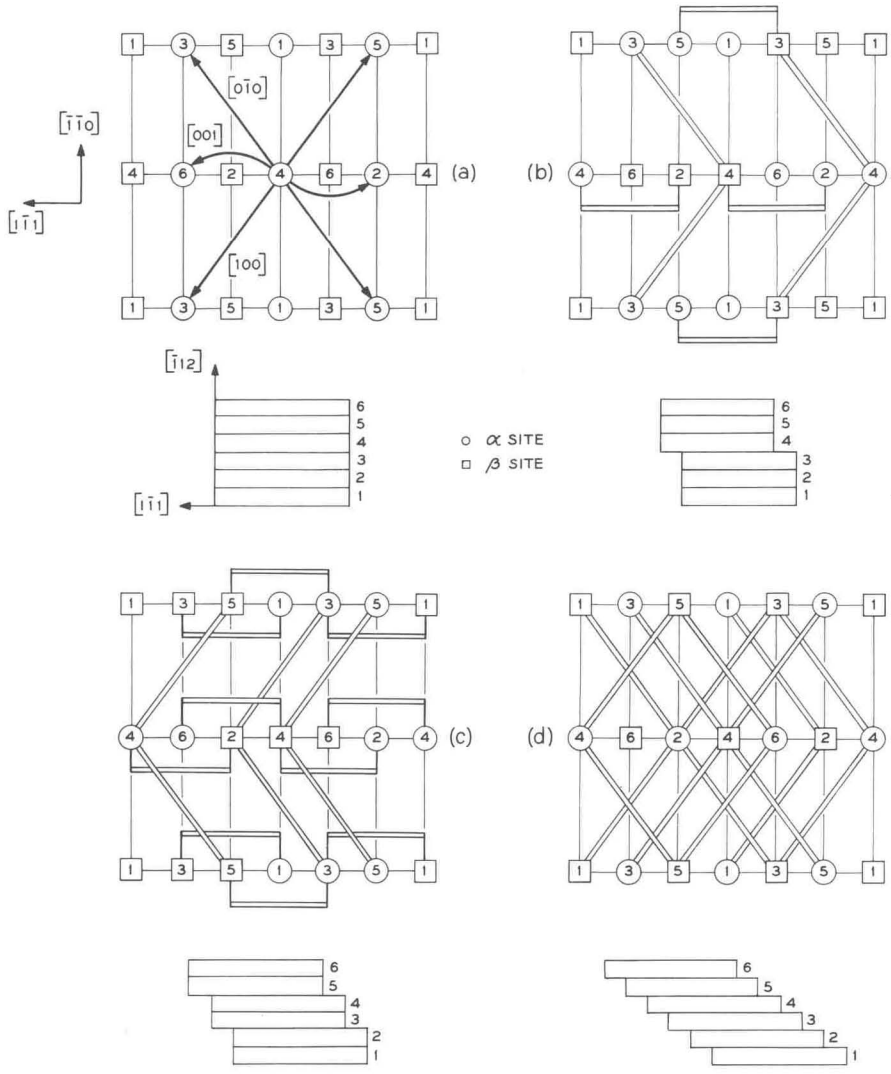

Fig. 6. Same as Fig. 5, except that emphasis is on *next-nearest-neighbor* pairs. (a) Undeformed state; all three ⟨100⟩ NNN directions contain AA and BB pairs only. (b) to (d) Alternative arrangements after ($\bar{1}$12) [1$\bar{1}$1] slip, showing AB pairs (double bars) induced in all three ⟨100⟩ directions.

Since ΔN_{BB} occurs in [111], [$\bar{1}$11] and [11$\bar{1}$], we have from eqn. (1)

$$\cos^2\varphi = (\cos^2\varphi_{[111]} + \cos^2\varphi_{[\bar{1}11]} + \cos^2\varphi_{[11\bar{1}]}) = -\tfrac{2}{3}(\alpha_1\alpha_2 - \alpha_2\alpha_3 + \alpha_3\alpha_1)\,, \quad (15)$$

which means that the [1$\bar{1}$1] slip direction is the effective direction of unlike pairs, which is a hard direction of magnetization for FeCo. In the general case, where the slip direction of slip system i has the direction cosines d_{1i}, d_{2i}, d_{3i},

$$\cos^2\varphi_i = -2(d_{1i}d_{2i}\alpha_1\alpha_2 + d_{2i}d_{3i}\alpha_2\alpha_3 + d_{3i}d_{1i}\alpha_3\alpha_1) \equiv -2f_i(\alpha_1, \alpha_2, \alpha_3)\,. \quad (16)$$

The insertion of eqns. (14) and (16) into eqn. (1) then leads to

$$E = -\tfrac{1}{2}Nlp_0p's^2\sum_i |S_i| f_i(\alpha_1, \alpha_2, \alpha_3)\,. \quad (17)$$

(*b*) *Short-range order case*

For the short-range order case, the two nearest-neighbor bonds associated with each ⟨111⟩ direction (in a unit cell) contain a total of $(1-\sigma)/2$ BB pairs in the undeformed state (see Appendix). After slip, $\sigma = 0$ for the 3⟨111⟩ directions other than the slip direction. Hence the gain in BB pairs in each of these directions is $\sigma/2$, or $\sigma/2a^2\sqrt{6}$ per

TABLE III: VALUES OF ε AND d (REFERRED TO CUBIC AXES) FOR THE TWELVE $\{112\}\langle 111\rangle$ SLIP SYSTEMS

No. of slip system	*Slip plane*	*Slip direction*	$2\varepsilon_{xx}$	$2\varepsilon_{yy}$	$2\varepsilon_{zz}$	$4\varepsilon_{yz}$	$4\varepsilon_{zx}$	$4\varepsilon_{xy}$	$3d_1d_2$	$3d_2d_3$	$3d_3d_1$
1	$(11\bar{2})$	111	S_1	S_1	$-2S_1$	$-S_1$	$-S_1$	$2S_1$	1	1	1
2	$(1\bar{2}1)$	111	S_2	$-2S_2$	S_2	$-S_2$	$2S_2$	$-S_2$	1	1	1
3	$(\bar{2}11)$	111	$-2S_3$	S_3	S_3	$2S_3$	$-S_3$	$-S_3$	1	1	1
4	(112)	$11\bar{1}$	S_4	S_4	$-2S_4$	S_4	S_4	$2S_4$	1	-1	-1
5	$(\bar{1}21)$	$11\bar{1}$	$-S_5$	$2S_5$	$-S_5$	$-S_5$	$2S_5$	S_5	1	-1	-1
6	$(2\bar{1}1)$	$11\bar{1}$	$2S_6$	$-S_6$	$-S_6$	$2S_6$	$-S_6$	S_6	1	-1	-1
7	$(1\bar{1}2)$	$\bar{1}11$	$-S_7$	$-S_7$	$2S_7$	S_7	$-S_7$	$2S_7$	-1	1	-1
8	(211)	$\bar{1}11$	$-2S_8$	S_8	S_8	$2S_8$	S_8	S_8	-1	1	-1
9	$(12\bar{1})$	$\bar{1}11$	$-S_9$	$2S_9$	$-S_9$	S_9	$2S_9$	$-S_9$	-1	1	-1
10	$(21\bar{1})$	$1\bar{1}1$	$2S_{10}$	$-S_{10}$	$-S_{10}$	$2S_{10}$	S_{10}	$-S_{10}$	-1	-1	1
11	(121)	$1\bar{1}1$	S_{11}	$-2S_{11}$	S_{11}	S_{11}	$2S_{11}$	S_{11}	-1	-1	1
12	$(\bar{1}12)$	$1\bar{1}1$	$-S_{12}$	$-S_{12}$	$2S_{12}$	$-S_{12}$	S_{12}	$2S_{12}$	-1	-1	1

TABLE IV: SUMMARY OF RESULTS BASED ON $\{112\}\langle 111\rangle$ SLIP

Rolling plane	*Rolling direction*	*Active slip systems*	$\lvert S_i\rvert$	E_{NN}	*Easy* axis*
(001)	$[\bar{1}10]$	7,12	$r/2$	$\left(\frac{E_1 r}{6}\right)\alpha_1\alpha_2$	TD
(115)	$[\bar{1}10]$	4,7,8,11,12	$\lvert S_4\rvert = 2r/27$ $\lvert S_8\rvert = \lvert S_{11}\rvert = 6r/27$ $\lvert S_7\rvert = \lvert S_{12}\rvert = 21r/54$	$\left(\frac{E_1 r}{162}\right)(31\alpha_1\alpha_2+2\alpha_2\alpha_3+2\alpha_3\alpha_1)$	TD
(112)	$[\bar{1}10]$	4,7,8,11,12	$r/3$	$\left(\frac{E_1 r}{18}\right)(3\alpha_1\alpha_2+\alpha_2\alpha_3+\alpha_3\alpha_1)$	RPN
(111)	$[\bar{1}10]$	4,7,8,11,12	$\lvert S_4\rvert = 2r/3$ $\lvert S_8\rvert = \lvert S_{11}\rvert = 2r/9$ $\lvert S_7\rvert = \lvert S_{12}\rvert = 7r/18$	$\left(\frac{E_1 r}{54}\right)(5\alpha_1\alpha_2+6\alpha_2\alpha_3+6\alpha_3\alpha_1)$	RPN
(110)	$[\bar{1}10]$	1,4,7,12	$r/2$	0	—

* Relative among the three symmetry directions of rolled strip. TD-transverse direction, RPN-rolling plane normal.

unit $\{112\}$ area. To this quantity we multiply by a factor $(p'|S|/d = p'|S|\sqrt{6}/a)$ as before, leading to the expression

$$\Delta N_{BB} = p'|S|\left(\frac{\sqrt{6}}{a}\right)\left(\frac{\sigma}{2a^2\sqrt{6}}\right) = \tfrac{1}{4}Np'\sigma|S| \,. \qquad (18)$$

Insertion of eqns. (16) and (18) into eqn. (1) then leads to

$$E = -\tfrac{1}{2}Nlp'\sigma\sum_i |S_i| f_i(\alpha_1,\alpha_2,\alpha_3) \qquad (19)$$

for the SRO case.

Finally, by combining the LRO and SRO expressions of eqns. (17) and (19), we obtain

$$E = -\tfrac{1}{2}E_1\sum_i |S_i| f_i(\alpha_1,\alpha_2,\alpha_3)\,, \qquad (20)$$

where $E_1 = Nlp'(p_0 s^2+\sigma)$ as before. Equation (20) is the expression for the slip-induced anisotropy energy developed by $\{112\}\langle 111\rangle$ slip and based on NN interactions.

(c) *Applications to rolling*

As in the treatment of $\{110\}\langle 111\rangle$ slip in Part 2 above, eqn. (20) has been applied to rolling of $(001)[\bar{1}10]$, $(115)[\bar{1}10]$, $(112)[\bar{1}10]$, $(111)[\bar{1}10]$ and $(110)[\bar{1}10]$ orientations. For the convenience of calculations, the appropriate parameters (similar to

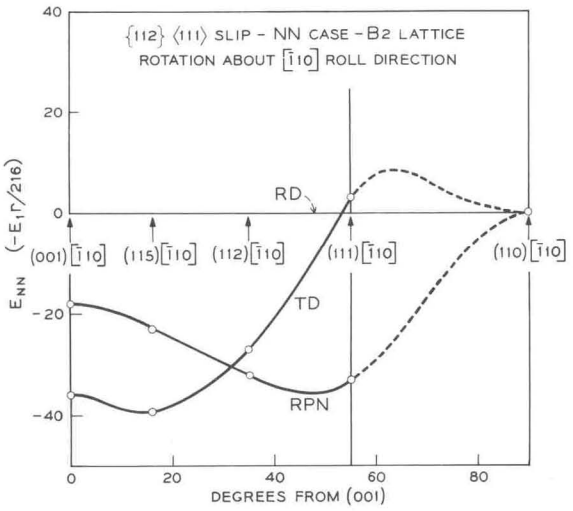

Fig. 7. Same as Fig. 3, except that calculations are based on *nearest-neighbor* interactions for the case of {112} ⟨111⟩ slip.

those of Table I) are listed in Table III. It may be noted that in determining the operating slip systems for a given crystal orientation, an equivalent Bishop and Hill method has not been developed for {112}⟨111⟩ slip. The procedure used here is based on the principle of minimum shear adopted by Taylor[15], the results of which are equivalent to the Bishop and Hill method. In the Taylor method, various combinations of glide-shears (from different slip systems) which satisfy the imposed (rolling) strain are obtained by trial; the combination(s) selected is one in which the sum of the absolute value of the glide-shears is a minimum. Since the number of slip system combinations is large, no attempt was made here to consider all of them. Instead, a judicious selection of the most likely combinations was tried; hence the results should approximate very closely (if not exactly) to the minimum shear condition*.

The results of the calculations are summarized in Table IV, with the anisotropy energies in the three symmetry directions of a rolled strip plotted in Fig. 7. It can be seen from Fig. 7 that the rolling direction is the highest energy or hardest direction, as required by the observed results of Fahlenbrach *et al.*

In Fig. 8 we combine Figs. 3 and 7 for the case of mixed {110}⟨111⟩ and {112}⟨111⟩ slip, with contributions of 50 and 75% {112}⟨111⟩ shown. It may be noted that if RD, TD and RPN are to be arranged in the order of decreasing energy as implied by Fahlenbrach's observations, Fig. 8 indicates that more than about 60% of the deformation is taken up by {112}⟨111⟩ slip. If the weaker NNN interactions (Fig. 4) are included, this value would be somewhat higher.

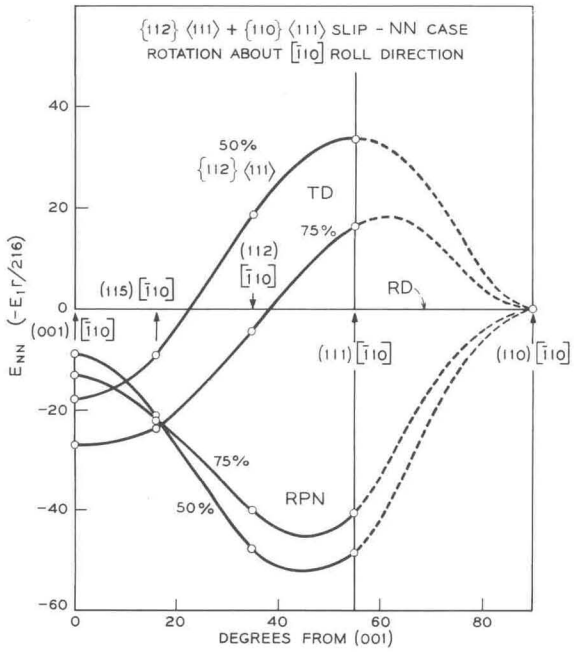

Fig. 8. Figures 3 and 7 combined, for the case of mixed {110} ⟨111⟩ + {112}⟨111⟩ slip. Curves shown are for 50% and 75% {112}⟨111⟩ slip. Note that the average energy from (001) [1̄10] to (111)[1̄10] is lowest for RPN, and TD has lower average energy than RD for greater than about 60% {112} ⟨111⟩ slip.

4. DISCUSSION

While the present theory is capable of explaining the observed results in the polycrystalline material, tests on single crystals are less ambiguous. Such tests can be done conveniently with magnetic torque measurements of disks cut out of the rolling plane. Figure 8 shows that in the (001)[1̄10] orientation, RD is a harder direction than TD. As the orientation rotates away, the rolling plane becomes isotropic in the vicinity of (112) [1̄10],

* *Note added in proof* (12–5–66): Since this paper was written, the complete Taylor analysis for {112} ⟨111⟩ slip has been performed by a computer method. The computer results confirmed that the operating slip systems determined by the previous less rigorous method truly conformed to the minimum shear condition. Thus the uncertainties expressed in Section 3(3) are removed. (The author is grateful to Mrs. W. L. Mammel and Mrs. G. Souren for the computer programming.)

beyond which TD becomes a harder direction. Finally, the rolling plane becomes isotropic again at (110)[$\bar{1}$10]. In these single crystal studies, two points need to be considered. First, because of lattice rotations that may accompany the deformation, the results on heavily rolled samples may need to take into account such changes in crystal orientation. From the polycrystalline texture analogy, the most stable orientations are from (100) [$\bar{1}$10] to (112) [$\bar{1}$10]. Secondly, the analysis is based on plane strain deformation. For some orientations, notably (110)[$\bar{1}$10], the disposition of the slip systems is such that the crystal tends to widen. In this case, ordinary rolling procedures may become inadequate. To insure negligible width change, a better method is to deform the crystal in a simple plane strain compression fixture which consists of a channel formed by die blocks[16]. In addition, this method allows a more homogeneous deformation, ready examination of slip lines, and accurate alignment of orientation even for small crystals. The latter feature may be especially important in FeCo, where the α–γ solid state transformation has so far prevented successful growing of large single crystals.

The possibility exists, of course, with studies on other ferromagnetic alloys that exhibit the $B2$ superlattice. Such alloys are few indeed, at least in the binary systems. The alloy FeRh may be the only suitable candidate besides FeCo.

According to Kouvel and Hartelius[17], this alloy undergoes an antiferromagnetic–ferromagnetic transition on heating to about 350°K. The structure in both cases is $B2$. Except for possible complications from the magnetic transition, there is no reason why slip-induced directional order could not be studied in the ferromagnetic state. Such a study should reveal the sign of the coefficient l of the pseudo-dipolar coupling energy (see eqn. (1)) for FeRh.

A further note regarding the present theory concerns the possible developments of other types of magnetic anisotropy during rolling. One of these is the magnetocrystalline anisotropy. Since preferred orientation is obtained on rolling, crystal anisotropy could be a factor. The results on the 2% V–FeCo alloy[6] indicate that the cold-worked induced anisotropy almost disappears after annealing at 500–600°C. Since the recrystallization temperature for this alloy is about 700°C*, the deformation texture is not expected to change after such an anneal. On the other hand, it probably converts the disordered (cold-worked) matrix to a long-ranged ordered state. According to Hall[21], the crystal anisotropy constant $K_1 \approx -2 \times 10^5$ ergs/cm^3 for the disordered alloy and decreases with ordering, which could then explain the corresponding decrease of the observed anisotropy after the 500–600°C anneal. However, a large negative value of K_1 in the cold-rolled state implies the $\langle 111 \rangle$ direction as the easy axis of magnetization. There is then difficulty of explaining why the rolling plane normal, which consists of a rotational spread from $\{100\}$ to $\{111\}$ (see Fig. 2), is the especially easy axis as observed. Studies in the vicinity of 42–45% Co, where $K_1 \approx 0$ in the disordered state[21], should further elucidate the role of crystal anisotropy in rolled material.

A second source of anisotropy in the rolled material is magnetostrictive anisotropy. Because of the large magnetostriction of FeCo, the residual stress that remains after rolling could lead to a substantial magnetostrictive anisotropy energy. The residual stress pattern and its effect on the overall magnetic anisotropy remain unclear. Unless a stress is uniformly directed throughout the material (such as by applying a tensile or compressive force), it is not expected to result in a large overall anisotropy. Experiments indicate that the rolled anisotropy in nickel, a relatively magnetostrictive material, is nil[22,23] or at most 10^2 ergs/cm^3 (ref. 3). Assigning the latter value to magnetostrictive anisotropy and adjusting for the larger magnetostriction in FeCo (2–3 times over Ni), one is still far from the observed anisotropy energy of 10^5 ergs/cm^3 observed in rolled FeCo[7,8].

SUMMARY

The slip-induced directional order theory has been developed for the $B2$-type superlattices. The theory is then applied to calculate the magnetic anisotropy obtained by rolling of single crystals near the FeCo composition. The results of analyses on orientations which comprise the crystallographic texture spread of the rolled polycrystalline material are

* Although this temperature was actually obtained with the binary FeCo alloy[18,19], no appreciable change from the small vanadium addition is expected. According to English[20], the ordering reaction, which appears responsible for the high recrystallization temperature of FeCo[18,19], is essentially complete after a few seconds of annealing at 565°C in the 2% V–FeCo alloys.

compared with the observations of Fahlenbrach and co-workers. It is concluded that the observed anisotropy can be rationalized in terms of the slip-induced directional order theory.

ACKNOWLEDGEMENTS

The author wishes to thank A. T. English and J. H. Wernick for valuable discussions.

APPENDIX

1. CALCULATION OF BB-PAIRS RESULTING FROM $\{110\}\langle 111\rangle$ SLIP IN A $B2$ STRUCTURE

(a) *Long-range order — nearest-neighbor case*

The long-range ordered $B2$ structure, Fig. 1(a), consists of two simple cubic sublattices α and β. The total number of BB nearest-neighbor atom pairs in any direction is given by

$$N_{BB} = N_{\alpha\beta}P_{BB}(\alpha\beta) + N_{\alpha\alpha}P_{BB}(\alpha\alpha) + N_{\beta\beta}P_{BB}(\beta\beta), \quad \text{(A1)}$$

where $N_{\alpha\beta}$, $N_{\alpha\alpha}$, and $N_{\beta\beta}$ are the number of bonds joining α and β, α and α, and β with β sites, respectively; and $P_{BB}(\alpha\beta)$, $P_{BB}(\alpha\alpha)$ and $P_{BB}(\beta\beta)$ are respectively the probabilities of a BB pair associated with $\alpha\beta$, $\alpha\alpha$, and $\beta\beta$ bonds.

From the definition of the Bragg and Williams LRO parameter s[24]

$$s = \frac{r_\alpha - x_A}{1-x_A} = \frac{r_\beta - x_B}{1-x_B}, \quad \text{(A2)}$$

where

r_α = fraction of α sites (rightly) occupied by A atoms

r_β = fraction of β sites (rightly) occupied by B atoms

x_A = fraction of A atoms in the lattice

x_B = fraction of B atoms in the lattice,

and the definitions

$w_\alpha = 1 - r_\alpha$ = fraction of α sites (wrongly) occupied by B atoms,

$w_\beta = 1 - r_\beta$ = fraction of β sites (wrongly) occupied by A atoms,

we have[25], for $x_A = x_B = \frac{1}{2}$,

$$\begin{aligned} P_{BB}(\alpha\alpha) &= w_\alpha^2 = \tfrac{1}{4}(1-s)^2 \\ P_{BB}(\beta\beta) &= r_\beta^2 = \tfrac{1}{4}(1+s)^2 \\ P_{BB}(\alpha\beta) &= w_\alpha r_\beta = \tfrac{1}{4}(1-s^2)\,. \end{aligned} \quad \text{(A3)}$$

In the undeformed condition, the distribution of bonds in any of the four nearest-neighbor $\langle 111\rangle$ directions of the two cells of Fig. 1(a), consists of $N_{\alpha\beta}=4$, $N_{\alpha\alpha}=N_{\beta\beta}=0$. Hence $N_{BB}=4P_{BB}(\alpha\beta)$ as calculated from eqn. (A1).

Consider now that a one-step slip has occurred on successive (110) planes in the $[\bar{1}11]$ direction, the configuration of Fig. 1(b) is obtained. In $[\bar{1}11]$ and $[1\bar{1}1]$, which lie on the slip plane, there is no change in pair distribution. Along $[\bar{1}\bar{1}1]$ or $[111]$, which connects the slip planes, the distribution is changed to $N_{\alpha\alpha}=N_{\beta\beta}=2$, $N_{\alpha\beta}=0$. Thus the number of BB pairs becomes $N_{BB}=2P_{BB}(\alpha\alpha)+2P_{BB}(\beta\beta)$. The increase in BB pairs in $[\bar{1}\bar{1}1]$ or $[111]$ as a result of slip is then

$$\begin{aligned} \Delta N_{BB} &= 2P_{BB}(\alpha\alpha) + 2P_{BB}(\beta\beta) - 4P_{BB}(\alpha\beta) \\ &= 2s^2 \end{aligned} \quad \text{(A4)}$$

upon application of eqns. (A3). Per unit (110) area, we have $\Delta N_{BB} = s^2/a^2\sqrt{2}$. A similar expression has been derived previously by Brown and Herman[26].

(b) *Short-range order — nearest-neighbor case*

In the short-range ordered lattice, the nearest-neighbor bonds are no longer identified by α and β sites. In this case, the number of BB pairs is given by

$$N_{BB} = n\langle P_{BB}\rangle \quad \text{(A5)}$$

where n is the number of bonds and $\langle P_{BB}\rangle$ is the average probability of a bond being a BB pair. The value of $\langle P_{BB}\rangle$ is obtained from the Bethe SRO parameter σ[25]:

$$\sigma = \frac{\langle P_{AB}\rangle - 2x_A x_B}{\langle P_{AB,max}\rangle - 2x_A x_B}, \quad \text{(A6)}$$

where $\langle P_{AB}\rangle$ is the average probability of a bond being AB, and $\langle P_{AB,max}\rangle$ is the value of $\langle P_{AB}\rangle$ at maximum order. For $x_A = x_B = \frac{1}{2}$, $\langle P_{AB,max}\rangle = 1$ and thus

$$\sigma = 2(\langle P_{AB}\rangle - \tfrac{1}{2}) \quad \text{(A7)}$$

The quantities $\langle P_{AB}\rangle$ and $\langle P_{BB}\rangle$ are related by the equation[17]

$$x_B = \langle P_{BB}\rangle + \tfrac{1}{2}\langle P_{AB}\rangle\,. \quad \text{(A8)}$$

Hence

$$\langle P_{BB}\rangle = \tfrac{1}{4}(1-\sigma)\,. \quad \text{(A9)}$$

In the two unit cells of Fig. 1(a), there are $4\langle P_{AB}\rangle = 1-\sigma$ BB pairs in any of the four $\langle 111\rangle$ directions.

After (110)[$\bar{1}$11] slip, Fig. 1(b), the distribution in [$\bar{1}$11] and [1$\bar{1}$1] remains unchanged. In [$\bar{1}\bar{1}$1] or [111], $\sigma=0$. Hence the number of BB pairs induced by slip is $\Delta N_{BB}=\sigma$, or $\sigma/2a^2\sqrt{2}$ per unit (110) area, in the [$\bar{1}\bar{1}$1] or [111] direction.

(*c*) *Long-range order — next-nearest-neighbor case*

There are three ⟨100⟩ next-nearest-neighbor directions. One of these, [001], lies on the slip plane, (110), and is not disturbed by slip. The other two, [010] and [100], will alter the atom pair distribution after slip.

In the two unit cells of Fig. 1(a), we have $N_{\alpha\alpha}=N_{\beta\beta}=2$, $N_{\alpha\beta}=0$ before slip, where $N_{\alpha\alpha}$ etc. are now referred to next-nearest-neighbor bonds. After slip, Fig. 1(b), $N_{\alpha\alpha}=N_{\beta\beta}=0$, $N_{\alpha\beta}=4$ in [010] or [100]. Hence the gain in BB pairs in either of these two directions is

$$\Delta N_{BB}=4P_{BB}(\alpha\beta)-2P_{BB}(\alpha\alpha)-2P_{BB}(\beta\beta)=-2s^2, \tag{A10}$$

or $-s^2/a^2\sqrt{2}$ per unit (110) area.

(*d*) *Short-range order — next-nearest-neighbor case*

For the next-nearest-neighbor case, the value of $\langle P_{AB,max}\rangle$ in eqn. (A6) is zero, as complete order results in like-atom pairs in all NNN bonds. We then have, from eqn. (A6),

$$\sigma_2=1-2\langle P_{AB}\rangle, \tag{A11}$$

with σ_2 denoting the SRO parameter for the NNN case. With the aid of eqn. (A8), eqn. (A11) becomes

$$\langle P_{BB}\rangle=\tfrac{1}{4}(1+\sigma_2). \tag{A12}$$

Thus, from Fig. 1(a), the number of BB pairs in [010] or [100] is $4\langle P_{BB}\rangle=1+\sigma_2$. After slip, $\sigma_2=0$. Hence the number of BB pairs gained by slip is $\Delta N_{BB}=-\sigma_2$, or $-\sigma_2/2a^2\sqrt{2}$ per unit (110) area.

2. CALCULATION OF BB-PAIRS RESULTING FROM {112} ⟨111⟩ SLIP IN A *B*2 STRUCTURE

(*a*) *Long-range order — nearest-neighbor case*

In the undeformed condition, there are two $\alpha\beta$ bonds per unit cell in each of four ⟨111⟩NN directions. After slip, these bonds change to an $\alpha\alpha$ bond and a $\beta\beta$ bond in the three ⟨111⟩ directions other than the slip direction. Hence $\Delta N_{BB}=P_{BB}(\alpha\alpha)+P_{BB}(\beta\beta)-2P_{BB}(\alpha\beta)$. When values of eqns. (A3) are entered, we obtain $\Delta N_{BB}=s^2$, or $s^2/a^2\sqrt{6}$ per unit {112} area.

(*b*) *Short-range order — nearest-neighbor case*

Here, in the undeformed state, the two bonds per cell in each ⟨111⟩ direction contribute $2\langle P_{BB}\rangle$ pairs of BB bonds. From eqn. (A9), $\langle P_{BB}\rangle=(1-\sigma)/4$. After slip, $\sigma=0$ and the gain in BB bonds is $\Delta N_{BB}=\sigma/2$, or $\sigma/2a^2\sqrt{6}$ per unit {112} area, in the three ⟨111⟩ directions other than the slip direction.

REFERENCES

1 S. CHIKAZUMI, K. SUZUKI AND H. IWATA, *J. Phys. Soc. Japan*, *12* (1957) 1259.
2 S. CHIKAZUMI, K. SUZUKI AND H. IWATA, *J. Phys. Soc. Japan*, *15* (1960) 250.
3 N. TAMAGAWA, Y. NAKAGAWA AND S. CHIKAZUMI, *J. Phys. Soc. Japan*, *17* (1962) 1256.
4 G. Y. CHIN, *J. Appl. Phys.*, *36* (1965) 2915.
5 G. Y. CHIN AND E. A. NESBITT, *J. Appl. Phys.*, *37* (1966) 1214.
6 E. HOUDREMONT, J. JANSSEN, G. SOMMERKORN AND H. FAHLENBRACH, *Tech. Mitt. Krupp*, *15* (1957) 13.
7 W. BARAN, W. BREUER, H. FAHLENBRACH AND K. JANSSEN, *Tech. Mitt. Krupp*, *18* (1960) 81.
8a H. FAHLENBRACH AND W. BARAN, *Z. Angew. Phys.*, *17* (1964) 178.
8b H. FAHLENBRACH, *Tech. Mitt. Krupp*, *23* (1965) 104.
9 W. C. ELLIS AND E. S. GREINER, *Trans. Am. Soc. Metals*, *29* (1941) 415.
10 N. S. STOLOFF AND R. G. DAVIES, *Acta Met.*, *12* (1964) 473.
11 L. NÉEL, *J. Phys. Radium*, *15* (1954) 225.
12 J. B. COHEN AND M. E. FINE, *J. Phys. Radium*, *23* (1962) 749.
13 J. F. W. BISHOP AND R. HILL, *Phil. Mag.*, *42* (1951) 414, 1298.
14 J. F. W. BISHOP, *Phil. Mag.*, *44* (1953) 51.
15 G. I. TAYLOR, *J. Inst. Metals*, *62* (1938) 307.
16 G. Y. CHIN, E. A. NESBITT AND A. J. WILLIAMS, *Acta Met.*, *14* (1966) 467.
17 J. KOUVEL AND C. HARTELIUS, *J. Appl. Phys.*, *33* (1962) 1343S.
18 M. M. BORODKINA, E. I. DETALF AND YA. P. SELISSKII, *Phys. Metals Metallog.*, *7* (2) (1959) 50.
19 YA. P. SELISSKII AND M. N. TOLOCHKO, *Phys. Metals Metallog.*, *13* (4) (1962) 98.
20 A. T. ENGLISH, *Trans. Met. Soc. AIME*, *236* (1966) 14.
21 R. C. HALL, *Trans. Met. Soc. AIME*, *218* (1960) 268.
22 G. W. RATHENAU AND J. A. SNOEK, *Physica*, *8* (1941) 555.
23 H. W. CONRADT AND K. SIXTUS, *Z. Physik*, *23* (1942) 39.
24 T. MUTO AND Y. TAKAGI, *Solid State Phys.*, *1* (1955) 194.
25 L. GUTTMAN, *Solid State Phys.*, *3* (1956) 145.
26 N. BROWN AND H. HERMAN, *Trans. AIME*, *206* (1956) 1353.

Printed in The Netherlands